Eur. Phys. J. A **18**, 283–287 (2003)
DOI 10.1140/epja/i2002-10217-3

THE EUROPEAN PHYSICAL JOURNAL A

# Progress in hypernuclear physics

T. Nagae[a]

High Energy Accelerator Research Organization (KEK), 1-1 Oho, Tsukuba, Ibaraki 305-0801, Japan

Received: 30 September 2002 /
Published online: 22 October 2003 – 

**Abstract.** The recent progress in hypernuclear physics is discussed in this paper. The topics include recent results on hypernuclear gamma-ray spectroscopy, non-mesonic weak decay, and double-$\Lambda$ hypernuclei. Future prospects at the 50 GeV PS are also discussed.

**PACS.** 21.80.+a Hypernuclei – 25.80.-e Meson- and hyperon-induced reactions

## 1 Introduction

Since the 1980s, the Alternating-Gradient Synchrotron (AGS) in Brookhaven National Laboratory (BNL) and the 12 GeV proton synchrotron (PS) in KEK have played a very important role in Hypernuclear Physics by providing high-intensity $K^-$ and $\pi^\pm$ beams. The $(\pi^+, K^+)$ and $(K^-, \pi^-)$ reactions were used for the production of $\Lambda$ hypernuclei, and the $(K^-, K^+)$ reaction for the investigation on the strangeness $S=-2$ systems, such as double-$\Lambda$ hypernuclei, $\Xi^-$ hypernuclei, and the hypothetical $H$ dibaryon. These experiments at BNL-AGS and KEK-PS have extended the scope of hypernuclear physics to the physics of hadron many-body systems with strangeness degrees of freedom, *i.e.* Strangeness Nuclear Physics.

Recently, Jefferson Laboratory (JLab) started hypernuclear spectroscopy with a different reaction of $(e, e'K^+)$. In 2007, the new 50 GeV proton synchrotron, now in construction in Japan, will be in operation. Then, it will be the opening of a new era in Strangeness Nuclear Physics.

## 2 Recent topics

### 2.1 Spectroscopy of Λ hypernuclei

The spectroscopy of $\Lambda$ hypernuclei has been successfully carried out in KEK by using the SKS spectrometer [1]. An overview of the measurements with the $(\pi^+, K^+)$ reactions was given in ref. [2]. The SKS spectrometer improved the energy resolution in $\Lambda$ hypernuclear spectroscopy from 3–4 $\mathrm{MeV_{FWHM}}$ to $\sim 2$ MeV, and further improved it to 1.45 MeV in the recent measurement [3]. The energy resolution resolved the major shell structure of $\Lambda$-orbits up to ${}^{208}_{\Lambda}\mathrm{Pb}$ [4] owing to the selectivity of the $(\pi^+, K^+)$ reaction due to the high-momentum transfer ($\sim 350$ MeV/$c$) of the reaction. It also revealed, for the first time, several core-excited states of ${}^{12}_{\Lambda}\mathrm{C}$ [4,3]. Some of them were not simply explained in naive weak-coupling structure, and it was suggested that the parity-mixing intershell couplings mediated by a $\Lambda$-particle should be taken into account [5].

The great progress in $\Lambda$ hypernuclear spectroscopy has taken place with a success of a hypernuclear $\gamma$-ray measurement by using a germanium (Ge) detector system, called Hyperball, in KEK [6]. The detector consisted of fourteen $N$-type coaxial Ge detectors of 60% relative efficiency. It covered 15% of the $4\pi$ sr. The energy resolution of 3–4 $\mathrm{keV_{FWHM}}$ was achieved at 1.33 MeV. It is a great improvement. So far, a few hypernuclear $\gamma$-rays were well-identified with NaI counters in worse energy resolutions.

The measurement observed the spin-flip $M1(\frac{3}{2}^+ \to \frac{1}{2}^+)$ $\gamma$-ray at 691.7±0.6(stat)±1.0(syst) keV in ${}^{7}_{\Lambda}\mathrm{Li}$, for the first time. The energy splitting provided a stringent constraint to the strength of the $\Lambda N$ spin-spin interaction.

It also observed the $E2(\frac{5}{2}^+ \to \frac{1}{2}^+)$ $\gamma$-ray transition at $2050.1 \pm 0.4$(stat)±0.7(syst) keV. Because of the good energy resolution of the Hyperball, we could measure the lifetime of the $\frac{5}{2}^+$ state from the peak shape analysis, the so-called Doppler-shift attenuation method [7]. The large momentum transfer of the $(\pi^+, K^+)$ reaction ($\sim 350$ MeV/$c$) makes the stopping time of the recoiling ${}^{7}_{\Lambda}\mathrm{Li}$ ($\sim 13$ ps) comparable to the expected lifetime (3–10 ps) of the $\frac{5}{2}^+$ state. The observed $\gamma$-ray peak at 2050 keV had two components; a sharp peak and a Doppler-broadened tail part. The sharp peak corresponds to the $\gamma$-rays emitted after the stopping of the recoiling ${}^{7}_{\Lambda}\mathrm{Li}$. From the two-component fitting by changing the lifetime of the $\frac{5}{2}^+$ state, the lifetime was obtained to be $5.8^{+0.9}_{-0.7} \pm 0.7$ ps, from which the reduced transition probability, $B(E2)$, was estimated to be $3.6 \pm 0.5^{+0.5}_{-0.4} e^2\,\mathrm{fm}^4$. This value is about one-third of the $B(E2)$ of the corresponding $E2(3^+ \to 1^+)$ transition in ${}^{6}\mathrm{Li}$. The $B(E2)$ is very sensitive to size contraction; in

[a] e-mail: tomofumi.nagae@kek.jp

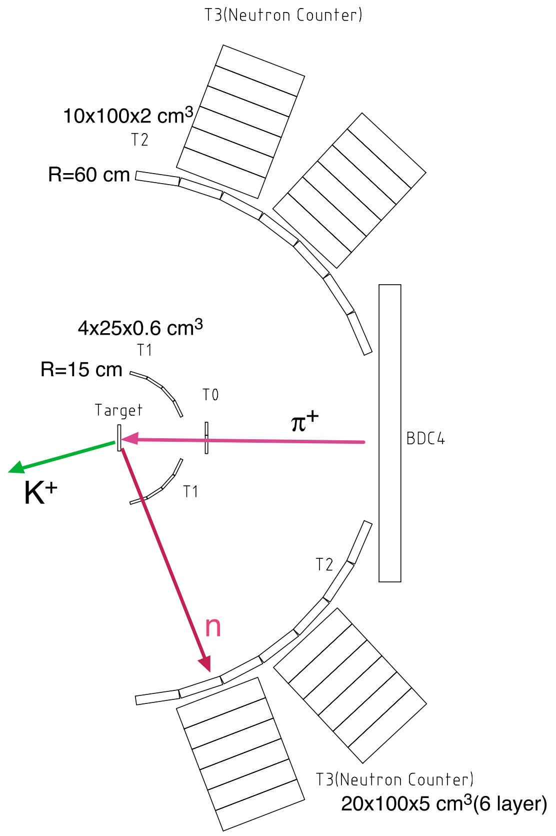


**Fig. 1.** Detector setup for the coincidence measurement of neutrons and protons emitted from non-mesonic weak decays in KEK-PS E369.

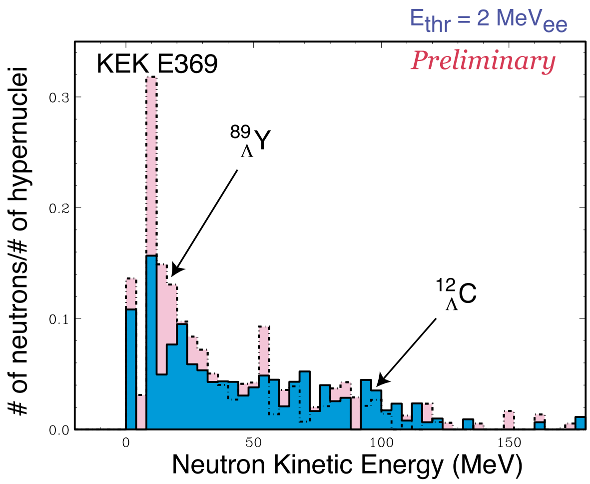


**Fig. 2.** The neutron energy spectra with a 2 MeV$_{ee}$ threshold for $^{12}_{\Lambda}$C and $^{89}_{\Lambda}$Y. The vertical scale is normalized to the number of hypernuclei in the bound region.

this case, the shrinkage of the $^6$Li core in the $^7_{\Lambda}$Li hypernucleus.

The further $\gamma$-ray measurements in $p$-shell $\Lambda$ hypernuclei are in progress at BNL-AGS with the $(K^-, \pi^-)$ reactions by using the Hyperball.

### 2.2 Weak decay of Λ hypernuclei

The weak decay properties of a $\Lambda$-hyperon in hypernuclei is another interesting subject. It is well known that the mesonic free $\Lambda$ decay($\Lambda \to \pi N$) is strongly suppressed because of the Pauli blocking and the dominant decay mode is the non-mesonic decay($\Lambda N \to NN, \Lambda NN \to NNN$). However, the present experimental data have too large ambiguities on the total decay rate and the neutron emission probability to pin down the reaction mechanism.

In the study of non-mesonic weak decays of $\Lambda$ hypernuclei, a large ratio of $\Gamma_n(\Lambda n \to nn)/\Gamma_p(\Lambda p \to np) \sim 1$ has been a puzzle not to be simply explained. The importance of two-nucleon–induced weak decay ($\Lambda NN \to NNN$) was suggested in ref. [8] related to this puzzle. However, available data were not enough to distinguish the one-nucleon–induced decay and two-nucleon–induced one. For example, the energy spectra of emitted nucleons should have different shapes in two decay processes [9]. An enhancement of the low-energy component is expected in the two-nucleon–induced process. The proton measurements so far done, however, usually had high energy thresholds of 40–50 MeV, which lost sensitivity to detect the low-energy component from the two-nucleon–induced process, if it existed. Therefore, we carried out the neutron measurement, in which the detection energy threshold could be reduced to $\leq$10 MeV. The quality of the neutron measurements so far has been very bad in statistics and signal-to-noise ratio.

The experimental setup for coincidence measurements of neutrons and protons emitted from non-mesonic weak decays of $^{89}_{\Lambda}$Y is shown in fig. 1. Since the mesonic weak-decay rate is expected to be negligibly small, all kinds of weak-decay products were measured in this setup.

The emitted timing of protons was measured with the T1 counter located 15 cm apart from the target. The flight time difference of protons was corrected with the velocity measured from the time of flight between the T1 and T2 counters. The overall timing resolution for protons was found to be $\sim$ 150 ps (rms).

Neutral particles, such as $\gamma$'s and neutrons, were measured in the T3 counter with T1 and T2 as veto counters. The T3 counter consisted of six layers of a plastic scintillator (BC420) of 20[W]×100[L]×5[T] cm$^3$. The velocity of a neutral particle was obtained with a time-of-flight measurement between T0 and T3 counters. The relative timing of all 24 neutron counters was adjusted with the prompt $\gamma$'s from the $(\pi^+, pX)$ reaction. The typical resolution for the prompt $\gamma$'s was $\sim$ 200 ps (rms).

The time-of-flight spectra of neutral particles in coincidence with bound states of $^{12}_{\Lambda}$C and $^{89}_{\Lambda}$Y showed that the $n/\gamma$ separation was very clean and we had a very good signal-to-noise ratio for neutrons. Gated to the neutron component, the energy spectra of neutrons from $^{12}_{\Lambda}$C and $^{89}_{\Lambda}$Y are obtained as shown in fig. 2.

Here, we notice that there exists no prominent bump structure around $\sim$ 75 MeV expected from the one-nucleon–induced decay process ($\Lambda N \to NN$) even for $^{12}_{\Lambda}$C, while the total shape seems to be very similar to that for the two-nucleon–induced process [9]. The recent measurement of the neutron spectrum from ${}^{5}_{\Lambda}$He [10] also shows a very similar shape with that for ${}^{12}_{\Lambda}$C. This suggests that rescattering effects after the one-nucleon–induced decay were unexpectedly large and/or the two-nucleon–induced decay plays a dominant role in the non-mesonic weak decay.

### 2.3 Double-Λ hypernuclei

There has been three emulsion events which showed the existence of double-$\Lambda$ hypernuclei [11–13]. However, these events had some ambiguities on interpretation etc., and the ground-state binding energy was not determined definitely.

In 2001, two new observations were reported from BNL-AGS and KEK-PS.

The KEK-PS E373 experiment [14] reported a double-hyperfragment event in a hybrid-emulsion measurement. The event is uniquely identified as the sequential decay of ${}^{6}_{\Lambda\Lambda}$He emitted from a $\Xi^-$ hyperon nuclear capture at rest,

$$
\begin{aligned}
{}^{12}\mathrm{C} + \Xi^- &\rightarrow {}^{6}_{\Lambda\Lambda}\mathrm{He} + {}^{4}\,\mathrm{He} + t\,,\\
{}^{6}_{\Lambda\Lambda}\mathrm{He} &\rightarrow {}^{5}_{\Lambda}\mathrm{He} + p + \pi^-.
\end{aligned}
$$

The binding energy of ${}^{6}_{\Lambda\Lambda}$He has been measured to be $7.25\pm0.19^{+0.18}_{-0.11}$ MeV, for the first time. It corresponds to the $\Delta B_{\Lambda\Lambda} = 1.01\pm0.20^{+0.18}_{-0.11}$ MeV, where $\Delta B_{\Lambda\Lambda}$ is defined by $\Delta B_{\Lambda\Lambda}({}^{A}_{\Lambda\Lambda}Z) = B_{\Lambda\Lambda}({}^{A}_{\Lambda\Lambda}Z) - 2B_{\Lambda}({}^{A-1}_{\Lambda}Z)$. It means the $\Lambda$-$\Lambda$ interaction is weakly attractive. Two of the past measurements gave a value of $\Delta B_{\Lambda\Lambda}$ to be about 4.5 MeV. Thus, the new value is smaller than these.

The other experiment at BNL-AGS [15] demonstrated the production of double-$\Lambda$ hypernuclei in the $(K^-, K^+)$ reaction on ${}^{9}$Be. It used a quite new technique to identify double-$\Lambda$ hypernuclei by using a Cylindrical Drift chamber System (CDS). In the CDS, two $\pi^-$'s emitted through sequential weak decays of hypernuclei were detected in a good momentum resolution. The result indicated the production of a significant number of the double-$\Lambda$ hypernucleus ${}^{4}_{\Lambda\Lambda}$H and the twin hypernuclei ${}^{4}_{\Lambda}$H and ${}^{3}_{\Lambda}$H.

## 3 Future prospects at the 50 GeV PS

The 50 GeV proton synchrotron (PS) is now under construction in the Joint Project between KEK and Japan Atomic Energy Research Institute (JAERI). The average beam current is 15.7 $\mu$A, which will produce the world's highest-intensity $K^-$ beams. The construction will be completed early in 2007.

In the experimental area for the slow-extracted beam, two secondary beam lines, K1.8 and K1.1, are proposed for the studies of strangeness nuclear physics; the former for the $S = -2$ systems, and the latter for the $S = -1$ systems.

A letter of intent for experiments on strangeness nuclear physics [16] well summarizes the initial experimental programs in this field. Among the various topics discussed in the letter of intent, I introduce two interesting programs: the investigation of new hadronic many-body systems with strangeness $S = -2$ and high-resolution $\gamma$-ray spectroscopy.

### 3.1 Spectroscopic study of S = −2 systems

The high-intensity $K^-$ beam at $\sim 1.8$ GeV/$c$ available at the 50 GeV PS is quite unique to open a new frontier of Strangeness Nuclear Physics in the spectroscopic studies of strangeness $S = -2$ systems. This is not only a step forward from the $S = -1$ systems as a natural extension, but also a significant step to explore the multi-strangeness hadronic systems; in the course of the limit, strange hadronic matter ($S = -\infty$) in the core of a neutron star is our concern. Also, it is important to extract some information on $\Xi N$ and $\Lambda$-$\Lambda$ interactions from the spectroscopic data.

The $(K^-, K^+)$ reaction is one of the best tools to implant the $S = -2$ through an elementary process $K^-+p \rightarrow K^++\Xi^-$, the cross-section of which in the forward direction has a broad maximum around this energy.

At present, the experimental information on the $S = -2$ systems mainly comes from several emulsion data in limited statistics. As for the $\Xi$ hypernuclei, there exist some hints of emulsion events for their existence. However, it is still not conclusive. Some upper limits on the $\Xi$-nucleus potential have been obtained from the production rate in the bound region of a $\Xi$ hypernucleus via the $(K^-, K^+)$ reaction.

The energy difference between the $(\Xi^- p)$ system and the $(\Lambda\Lambda)$ system is only 28.3 MeV in free space. Therefore, a relatively large configuration mixing between $\Xi^-+A$ and $\Lambda\Lambda+(A-1)$ states is suggested. It is very interesting to investigate whether the single-particle picture of $\Xi^-$ is valid or not in such a system.

It is expected that the spectroscopy of the $\Xi$ hypernuclei is promising. Here we use the $(K^-, K^+)$ reaction in which we can use the same method for the $(\pi^+, K^+)$ reaction in the $\Lambda$-hypernuclear spectroscopy. In fact, two reactions have very similar characteristics of large recoil momentum of a produced hyperon: $p_{\Xi^-} \sim 500$ MeV/$c$ and $p_\Lambda \sim 350$ MeV/$c$. Therefore, even for heavy targets well-separated peak structures are expected in spite of many possible excitations, because the spin-stretched configurations with $\ell_p + \ell_\Xi + J =$ even are strongly populated as in the case of the $(\pi^+, K^+)$ reaction, or more strongly.

For the spectroscopy of the $(K^-, K^+)$ reaction, we need two spectrometers as in the $(\pi^+, K^+)$ reaction: a beam line spectrometer for the incident $K^-$ and a $K^+$ spectrometer.

A 2 GeV/$c$ kaon beam line for the JHF was designed by J. Doornbos [17]. A beam line spectrometer is installed in the last part of the beam line. It consists of a QDQDQ system. It is estimated that the momentum resolution of $2\times10^{-4}$ could be achievable.

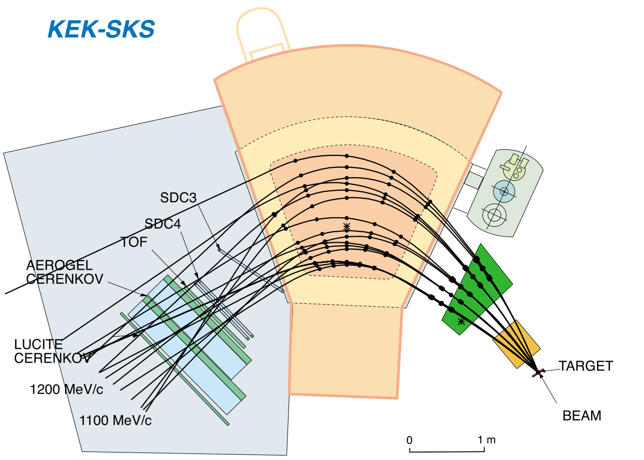


**Fig. 3.** Schematic layout of the SKS spectrometer for the ($K^-$, $K^+$) reaction at 1.65 GeV/$c$.

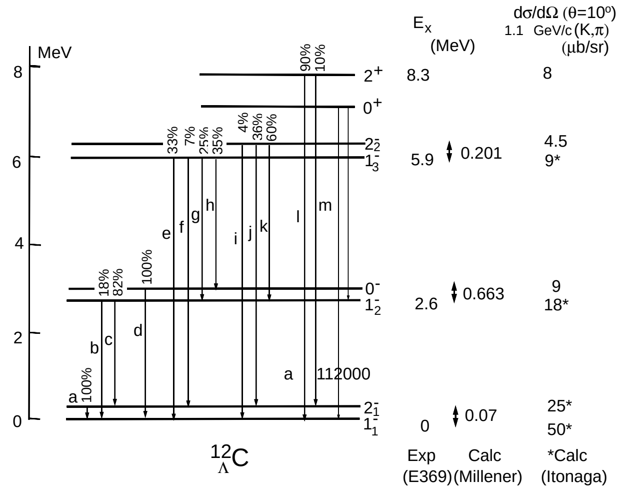


Expected Yield (5 days)

| single | | single | | γγ coincidnece with a | | γγ coincidnece with c | | γγ coincidnece with d | |
|---|---|---|---|---|---|---|---|---|---|
| a | 112000 | h | 1700 | c | 1900 | a | 1900 | h | 55 |
| b | 2600 | i | 64 | f | 50 | g | 39 | | |
| c | 12000 | j | 580 | g | 150 | k | 50 | | |
| d | 7500 | k | 1400 | j | 94 | | | | |
| e | 1100 | l | 2000 | k | 170 | | | | |
| f | 240 | m | 230 | m | 31 | | | | |
| g | 1300 | | | | | | | | |

**Fig. 4.** Top: Expected level energies and $\gamma$ transitions of $^{12}_{\Lambda}$C. Bottom: Expected yields of $\gamma$ transitions of $^{12}_{\Lambda}$C for 5 days' run. Yields of $\gamma$-$\gamma$ coincidence events are also shown.

For the $K^+$ spectrometer, we will use the existing SKS spectrometer with some modifications. In fig. 3, the setup of the SKS spectrometer for the ($K^-$, $K^+$) reaction is shown schematically.

Since the radius for the central momentum is larger than that for the ($\pi^+$, $K^+$) reaction, the target point is moved away from the magnet. So that, the acceptance of the spectrometer is reduced to be $\sim$ 50 msr. The overall energy resolution is estimated to be 2 MeV(FWHM) for a 2 g/cm$^2$ target thickness.

The production cross-section of the $\Xi$ hypernuclei in the ($K^-$, $K^+$) reaction is calculated to be $\sim 0.1$ $\mu$b/sr/MeV around the middle of the bound region for various types of potentials. Thus, the yield for the $^{208}$Pb target with 2 g/cm$^2$ thickness is estimated to be $\simeq$ 6 events/MeV/day. So, even for the heaviest case, we could get enough statistics within $\sim$ 20 days to obtain spectroscopic information. For lighter targets such as $^{28}$Si and $^{58}$Ni, the yields are several times higher with the normalized target thickness of 2 g/cm$^2$.

### 3.2 High-resolution hypernuclear $\gamma$-ray spectroscopy

High-resolution hypernuclear $\gamma$-ray spectroscopy will be extended further and exciting new physics fields will be opened up at the 50 GeV PS.

The ($K^-$, $\pi^-$) reaction at 1.1 GeV/$c$ is used in order to produce $\Lambda$ hypernuclei. This reaction has a large spin-flip amplitude and allows population of various hypernuclear states including spin-flip states with unnatural parities.

We require a secondary beam line whose intensity is optimized to 1.1 GeV/$c$. It should have a double-stage mass separator to obtain pure $K^-$ beams in order to minimize the counting rates of Ge detectors and tracking devices in the spectrometer. The beam intensity of 1.1 GeV/$c$ $K^-$ is expected to be $1.9 \times 10^7$ $K^-$ per spill ($2 \times 10^{14}$ protons) in 3.4 s cycle.

The momentum of the $K^-$ beam is measured event-by-event with a beamline spectrometer having $< 0.2$% FWHM resolution. The outgoing $\pi^-$ is measured with a spectrometer similar to SKS, which is required to have an acceptance of more than 50 msr and momentum resolution of $< 0.2$% FWHM. An overall mass resolution better than 3 MeV is necessary.

Around the target, we install a new Ge detector system, which is similar to the present Hyperball but has a much larger efficiency. In the present design, we expect to use 14 sets of "Segmented Super Clover Ge detectors", which has recently become commercially available. One detector set consists of four Ge crystals of 7 cm$\varnothing \times 14$ cm, and the electrode of each crystal is segmented into 4 read-out channels. Such a fine segmentation is necessary for Doppler-shift correction. The Ge crystals cover about 40% of the total solid angle. The Ge detector system has a photo-peak efficiency of 12% at 1 MeV in total. Each of the Ge detectors is surrounded by a set of BGO or GSO counters, which are used to veto Compton scattering and high-energy $\gamma$-rays from $\pi^0$.

An example of the $\gamma$-ray measurement in the case of $^{12}_{\Lambda}$C for 5-day data taking is shown in fig. 4. The production cross-sections of the $^{12}_{\Lambda}$C states (except for the first $2^+$ state) were calculated by Itonaga *et al.* for the 1.1 GeV/$c$ ($K^-$, $\pi^-$) reaction [18]. The energy levels are taken from the experimental values from KEK-E369 [3], but the doublet spacing energies are taken from the new parameter set of the spin-dependent interactions by Millener [19].

We will have quite enough yields for almost all the $\gamma$ transitions. We can expect good statistics even for $\gamma$-$\gamma$

coincidence spectra, which enable us to completely reconstruct the level scheme.

## 4 Summary

There has been a lot of progress in Hypernuclear Physics in the last decade. The recent success of hypernuclear $\gamma$-ray spectroscopy with the Hyperball detector opened a new stage of hypernuclear spectroscopy in precision. As for non-mesonic weak decays, new neutron spectra from several $\Lambda$-hypernuclei gave a new information to investigate the reaction mechanism. There was also important progress in double-$\Lambda$ hypernuclei.

We hope these efforts will be in full bloom at the 50 GeV PS with high-intensity $K^-$ beams.

## References


1. T. Fukuda *et al.*, Nucl. Instrum. Methods A **361**, 485 (1995).
2. T. Nagae, Nucl. Phys. A **691**, 76c (2001).
3. H. Hotchi *et al.*, Phys. Rev. C **64**, 044302 (2001).
4. T. Hasegawa *et al.*, Phys. Rev. C **53**, 1210 (1996).
5. T. Motoba, Nucl. Phys. A **639**, 135c (1998).
6. H. Tamura *et al.*, Phys. Rev. Lett. **84**, 5963 (2000).
7. K. Tanida *et al.*, Phys. Rev. Lett. **86**, 1982 (2001).
8. W.M. Alberico, A. De Pace, M. Ericson, A. Molinari, Phys. Lett. B **256**, 134 (1991).
9. A. Ramos, M.J. Vincente-Vacas, E. Oset, Phys. Rev. C **55**, 735 (1997).
10. H. Outa *et al.*, KEK E462 experiment, private communication.
11. D.J. Prowse, Phys. Rev. Lett. **17**, 782 (1966).
12. M. Danysz *et al.*, Nucl. Phys. **49**, 121 (1963).
13. S. Aoki *et al.*, Prog. Theor. Phys. **85**, 1287 (1991).
14. H. Takahashi *et al.*, Phys. Rev. Lett. **87**, 212502 (2001).
15. J.K. Ahn *et al.*, Phys. Rev. Lett. **87**, 132504 (2001).
16. JHF Strangeness Nuclear Physics Group, *Letter of Intent for Experiments on Strangeness Nuclear Physics at the 50-GeV Proton Synchrotron*, July 2000, unpublished, `http://www-jhf.kek.jp/JHF_WWW/LOI/50GeVNP-LOI-v1.0.pdf`).
17. J. Doornbos, KEK Report 97-5 (1997).
18. K. Itonaga *et al.*, Prog. Theor. Phys. Suppl. **117**, 17 (1994).
19. D.J. Millener, *Proceedings of the International Workshop on Hypernuclear Physics with Electromagnetic Probes (HYPJLAB99), Hampton, Virginia, 2-4 December, 1999.*